

Monoallelic Mutations in the Translation Initiation Codon of *KLHL24* Cause Skin Fragility

Yinghong He,^{1,13} Kristin Maier,^{1,13} Juna Leppert,¹ Ingrid Hausser,² Agnes Schwieger-Briel,^{3,4} Lisa Weibel,^{3,4} Martin Theiler,^{3,4} Dimitra Kiritsi,¹ Hauke Busch,^{5,6,7} Melanie Boerries,^{5,6,7} Katariina Hannula-Jouppi,^{8,9} Hannele Heikkilä,⁸ Kaisa Tasanen,¹⁰ Daniele Castiglia,¹¹ Giovanna Zambruno,¹² and Cristina Has^{1,*}

The genetic basis of epidermolysis bullosa, a group of genetic disorders characterized by the mechanically induced formation of skin blisters, is largely known, but a number of cases still remain genetically unsolved. Here, we used whole-exome and targeted sequencing to identify monoallelic mutations, c.1A>G and c.2T>C, in the translation initiation codon of the gene encoding kelch-like protein 24 (*KLHL24*) in 14 individuals with a distinct skin-fragility phenotype and skin cleavage within basal keratinocytes. Remarkably, mutation c.1A>G occurred de novo and was recurrent in families originating from different countries. The striking similarities of the clinical features of the affected individuals point to a unique and very specific pathomechanism. We showed that mutations in the translation initiation codon of *KLHL24* lead to the usage of a downstream translation initiation site with the same reading frame and formation of a truncated polypeptide. The pathobiology was examined in keratinocytes and fibroblasts of the affected individuals and via expression of mutant *KLHL24*, and we found mutant *KLHL24* to be associated with abnormalities of intermediate filaments in keratinocytes and fibroblasts. In particular, *KLHL24* mutations were associated with irregular and fragmented keratin 14. Recombinant overexpression of normal *KLHL24* promoted keratin 14 degradation, whereas mutant *KLHL24* showed less activity than the normal molecule. These findings identify *KLHL24* mutations as a cause of skin fragility and identify a role for *KLHL24* in maintaining the balance between intermediate filament stability and degradation required for skin integrity.

Inherited epidermolysis bullosa (EB) is a group of genetic disorders characterized by skin fragility and blister formation after trivial mechanical trauma.¹ In spite of the advanced knowledge of the molecular basis of EB and extensive genetic testing, a number of cases remain genetically unsolved.^{2–5} The most common EB type, EB simplex (MIM: 131800, 131960, 131760, 131900, 609352, and 601001), is mainly caused by monoallelic mutations in *KRT5* (MIM: 148040) and *KRT14* (MIM: 148066), which encode keratin 5 and keratin 14, respectively, the major intermediate filaments (IFs) expressed in basal keratinocytes of the epidermis. Most *KRT5* and *KRT14* mutations have a dominant-negative effect and weaken the mechanical resistance of keratin IFs in basal epidermal keratinocytes, resulting in skin cleavage within this epidermal layer.⁶ Furthermore, mutations in three other genes, *PLEC* (MIM: 601282), *DST* (MIM: 113810), and *EXPH5* (MIM: 612878), account for rare subtypes of basal EB simplex (MIM: 226670, 612138, 131950, 616487, 615425, and 615028).^{2,7–9}

Here, we combined deep phenotyping and whole-exome sequencing (WES) and identified monoallelic mutations in the translation initiation codon of *KLHL24* (MIM:

611295), encoding kelch-like protein 24 (*KLHL24*), in 14 individuals from ten families affected by genetically unsolved EB simplex. The families were unrelated and originated from Germany, Switzerland, Finland, Qatar, and Italy. The study included a total of 53 family members, 14 of whom had skin fragility, and 39 of whom were not affected. The clinical phenotype was remarkably consistent across all affected individuals and allowed for the prediction of a common genotype. In three families (A, B, and J), the inheritance was autosomal dominant, whereas the other seven families (C–I) showed simplex cases of disease (Table S1 and Figures 1 and S1). The clinical features changed with age, but all children and adults had similar cutaneous manifestations (compare Figures 1 and S2). Extensive skin defects were present on the extremities at birth (aplasia cutis congenita), leaving behind hypopigmentation and atrophy with a whirled pattern. Generalized blistering persisted during childhood and healed with cutaneous and follicular atrophy, linear and stellate scars, and hypopigmentation (Figures 1 and S2). Toenails were fragile and became progressively thicker. The cutaneous fragility decreased in adulthood. The adults had dyspigmentation and atrophy of the skin, scars, follicular

¹Department of Dermatology, University Medical Center Freiburg, Freiburg 79104, Germany; ²Department of Pathology, University of Heidelberg, Heidelberg 69120, Germany; ³Department of Paediatric Dermatology, University Children's Hospital Zurich, Zurich 8091, Switzerland; ⁴Department of Dermatology, University Hospital Zurich, Zurich 8091, Switzerland; ⁵Systems Biology of the Cellular Microenvironment Group, Institute of Molecular Medicine and Cell Research, Albert-Ludwigs-University Freiburg, Freiburg 79104, Germany; ⁶German Cancer Consortium (DKTK), German Cancer Research Center (DKFZ), Heidelberg 69120, Germany; ⁷Comprehensive Cancer Center Freiburg, Freiburg 79106, Germany; ⁸Department of Dermatology and Allergology, University of Helsinki and Helsinki University Hospital, Helsinki 00014, Finland; ⁹Folkhälsan Institute of Genetics, University of Helsinki, Helsinki 00014, Finland; ¹⁰Department of Dermatology, PEDEGO Research Unit, Medical Research Center Oulu, Oulu University Hospital and University of Oulu, Oulu 90014, Finland; ¹¹Laboratory of Molecular and Cell Biology, Istituto Dermopatico dell'Immacolata, Istituto di Ricovero e Cura a Carattere Scientifico, Rome 00167, Italy; ¹²Genetic and Rare Diseases Research Area, Bambino Gesù Children's Hospital, Istituto di Ricovero e Cura a Carattere Scientifico, Rome 00165, Italy

¹³These authors contributed equally to this work

*Correspondence: cristina.has@uniklinik-freiburg.de

<http://dx.doi.org/10.1016/j.ajhg.2016.11.005>.

© 2016 American Society of Human Genetics.

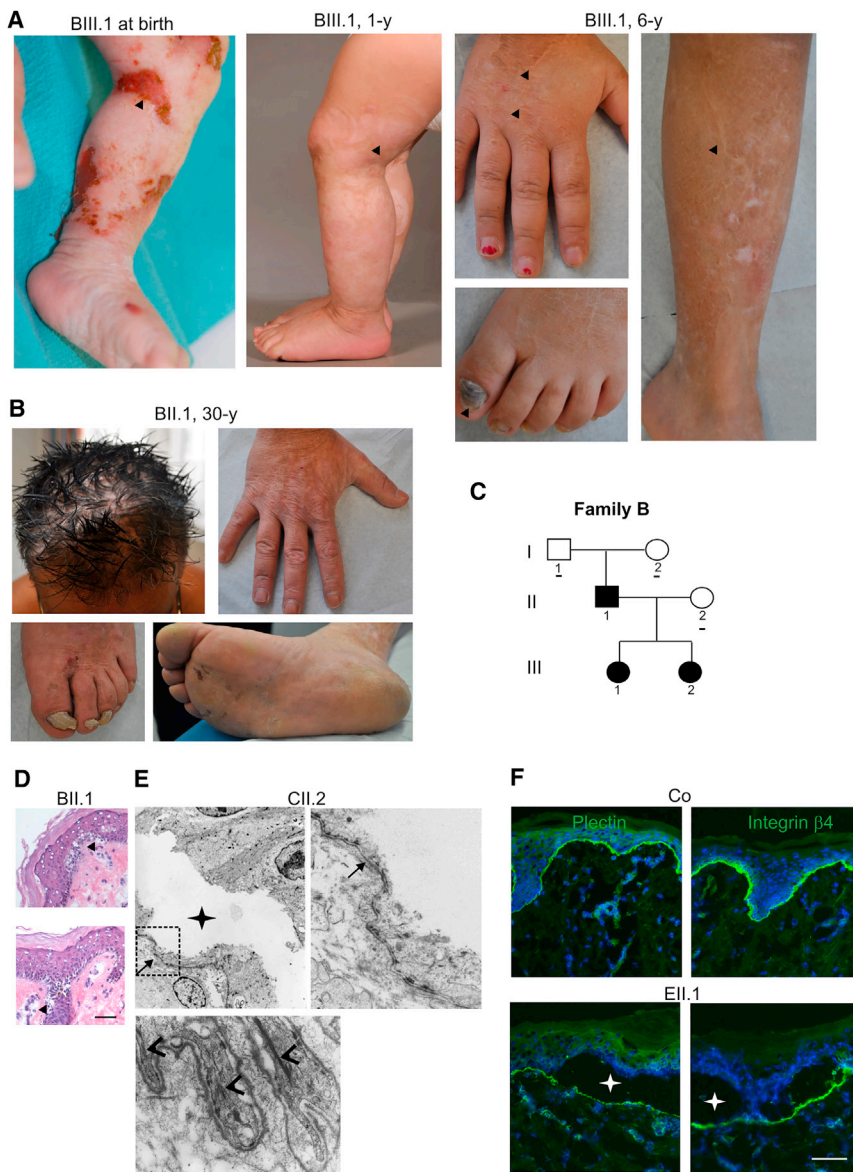


Figure 1. Clinical Features and Morphological Examinations of the Skin of Individuals with *KLHL24* Mutations

(A) Pictures of individual BIII.1 soon after birth and at 1 and 6 years of age demonstrate congenital skin defects, hypopigmentation with a whirled pattern, atrophy and linear scars on the dorsal aspects of the hands and on the lower legs, and thickened nails. Arrowheads point to the clinical features mentioned above.

(B) Pictures of individual BII.1 show sparse scalp hair, skin atrophy, palmoplantar keratoderma, and onychogryphosis of the toenails.

(C) Pedigree of family B. Dashes indicate that the mutation was excluded.

(D) H&E staining of skin sections obtained from the unblistered skin of BII.1 after rubbing demonstrates cleavage at the level of basal keratinocytes, which seem to lyse and loose adhesion (arrowheads). Scale bar represents 50 μ m.

(E) TEM micrographs of skin samples of CII.2. The upper panels demonstrate cleavage deep in the basal epidermal keratinocytes, just above the hemidesmosomes. Lamina densa of the basement membrane is indicated by arrows. The right panel is a 4-fold magnification of the marked area.

The lower panel shows keratin IFs (arrows). (F) Immunofluorescence staining of plectin and integrin β 4 in control skin (Co) and in skin sections obtained from EII.1. Note the presence of the markers at the blister base. Blisters are indicated by asterisks. Scale bar represents 50 μ m.

atrophy, sparse body hair, progressive diffuse alopecia of the scalp, diffuse palmoplantar keratoderma, and nail changes (shown in Figures 1 and S2 and summarized in Table S1). The unique characteristics of this phenotype were hair loss and follicular and cutaneous atrophy and scarring, features that are not present in persons with classic forms of EB simplex.

The study was performed according to a protocol approved by the ethics committee of the University of Freiburg, and written consent was obtained prior to sample collection. DNA from blood and cultured cells was obtained with the QIAmp DNA Mini Kit (QIAGEN). Skin biopsies of the index subjects and healthy individuals who underwent surgery were obtained after informed written consent was provided and were used for morphological analyses and cell isolation.

The classification as EB simplex was based on the level of skin cleavage, which was determined by H&E or transmis-

sion electron microscopy (TEM) (in individuals AII.2, CII.2, FIII.2, I II.1, and JII.2) or by immunofluorescence staining of markers of the dermal-epidermal junction (DEJ)¹⁰ (in AII.2, BII.1, BIII.1, CII.2, DIII.1, EII.1, FIII.2, GII.1, HII.1, and JII.2). In the skin samples of all index subjects, splits were found at the level of basal keratinocytes (Figures 1D–1F). The ultrastructural level of cleavage was located above the hemidesmosomes, close to the basement membrane. The morphology of the keratin IFs, the hemidesmosomes, and the basement membrane appeared normal (Figure 1E). Hemidesmosomal proteins, plectin, and integrin β 4 stained at the floor of the blisters (Figure 1F), and the staining intensity of the DEJ markers was comparable to that of control skin.

In a candidate approach, genes involved in EB were sequenced in all index subjects, but no pathogenic changes were found. WES was then employed in families A (affected mother AII.2 and daughter AIII.1; and unaffected parents AI.1 and AI.2), B (affected siblings BIII.1 and BIII.2), and E (affected EII.1 and unaffected parents). WES was performed by BGI with the AgilentSureSelect All Exon Kit on the Illumina HiSeq 4000 platform. Reads

were aligned to the human reference sequence (UCSC Genome Browser hg19) with the Burrows-Wheeler Aligner and trimmed to targeted intervals with Picard.^{11,12} Of the total effective bases, 55.40% mapped to target regions (capture specificity). The mean sequencing depth in target regions was 130.50 \times . On average, per sequencing individual, 99.90% of targeted bases had at least 1 \times coverage, and 99.10% had at least 10 \times coverage. All genomic variations, including SNPs and indels, were detected by state-of-the-art software, such as the Genome Analysis Toolkit HaplotypeCaller (v.3.3.0). After that, the hard-filtering method was applied to produce high-confident variant calls. Then, the AnnoDB tool developed by BGI was applied to perform a series of annotations for variants. The final variants and annotation results were used in the downstream advanced analysis. Under the assumption of dominant inheritance or de novo mutations, variants were filtered as follows: (1) variants in genes known to be associated with EB or candidate genes from mouse models were first verified, (2) common and synonymous variants were eliminated (>1% in dbSNP, 1000 Genomes, the NHLBI Exome Sequencing Project [ESP] Exome Variant Server, and/or the Exome Aggregation Consortium [ExAC] Browser), (3) predicted pathogenic heterozygous variants present in affected and absent in unaffected individuals were selected, and finally, (4) variants or genes present in all affected individuals of the three unrelated families were retained for validation. This strategy excluded mutations in any known EB-associated genes and revealed two heterozygous mutations in the start codon of *KLHL24* (GenBank: NM_017644.3 and NC_000003.12): c.1A>G (p.Met1?) in the affected members of families A and B and c.2T>C (p.Met1?) in the index subject of family E (Figures 2A and 2B). The mutations were validated by Sanger sequencing (primers and details are provided in Table S2). Furthermore, c.1A>G (p.Met1?) was disclosed in a heterozygous state in all affected individuals of families C, D, and F–J but in none of the unaffected relatives. Importantly, by testing a total of 53 individuals, including the healthy parents of the index subjects, we provide clear evidence that mutations perfectly segregated with the phenotype in each family and occurred de novo (Figures 1C, 2A and 2B, and S1).

Variants c.1A>G and c.2T>C were absent in cohorts of healthy control subjects in dbSNP, 1000 Genomes, the Exome Variant Server, and the ExAC Browser. They were predicted to change the Kozak consensus sequence and shift the start codon of *KLHL24*. For both c.1A>G and c.2T>C, the prediction of Mutation Taster¹³ was “disease causing” with a probability of 0.99. As a consequence, a downstream translation initiation site with the same reading frame resulting in a 28-aa-shortened sequence was predicted in silico (Figure 2C). This hypothesis was experimentally verified by recombinant expression of normal and mutant *KLHL24* cDNA. For validation of the results and better separation by SDS-PAGE, we designed both full-length and short forms of recombinant

KLHL24. In brief, full-length *KLHL24* cDNA (from cDNA position 1 to the penultimate codon) and the short form (from cDNA position 1 to position 409, corresponding to the first 136 codons) were amplified by PCR with REDTaq DNA Polymerase (Sigma-Aldrich) (the specific primers are listed in Table S2). The PCR products were cloned into the pcDNA3.1/CT-GFP-TOPO vector, and competent DH5 α *E. coli* (Thermo Fisher Scientific) were transformed according to the manufacturer's instructions. Plasmids encoding mutant *KLHL24* were obtained by site-directed mutagenesis with the QuikChange II Kit (Agilent Technologies), specific primers (Table S2), and the pcDNA3.1-*KLHL24* constructs as templates. Site-directed mutagenesis was performed according to the manufacturer's instructions. Positive clones were validated by control PCR, and sequencing and plasmid DNA was isolated with the Plasmid Maxi Kit (QIAGEN). HEK293 cells were grown in DMEM and transfected with the Superfect Transfection Reagent (QIAGEN) according to the manufacturer's protocol. Protein lysates (25 mM Tris-HCl, pH 7.5, 100 mM NaCl, 1% NP-40, 1 mM PEFA-Bloc, 10 mM EDTA, and protease inhibitor cocktail) were obtained 48–72 hr after transfection and used for SDS-PAGE and immunoblot with antibodies to GFP and GAPDH. In agreement with the prediction, recombinant expression of normal and mutant *KLHL24* cDNA in HEK293 cells confirmed that mutations c.1A>G and c.2T>C were translated into shorter truncated polypeptides, suggesting that Met29 was used for the initiation of translation: p.Val2_Met29del (Figure 2D).

Very little is known about *KLHL24*, which encodes *KLHL24*, and no related human disease has been reported so far. *KLHL24* has been shown to form homodimers and to regulate the function of kainate receptors in neurons,^{14,15} but it has not yet been linked to epidermal integrity. *KLHL24* belongs to the BTB/kelch family, which comprises a large group of highly conserved proteins involved in diverse cellular functions, including cytoskeleton interactions, nuclear transcription, and ubiquitination.^{16–18} In the N terminus, BTB (bric a brac 1, tramtrack, and broad) domains facilitate dimerization and protein binding. In particular, BTB domains bind to cullins, E3 ligase adapters, to target substrates for ubiquitin-dependent degradation by the 26S proteasome.^{19,20} N-terminal truncation due to the mutations in the translation initiation codon of *KLHL24* can affect functions of this region, such as dimerization and protein interactions, thus having a dominant-negative effect. Kelch domains form a tertiary structure of β -propellers, which have a role in binding to specific proteins targeted for degradation.¹⁸ One of the best-known *KLHL* proteins, *KLHL19* (also known as Keap1, encoded by *KEAP1* [MIM: 606016]), is an oxidative-stress sensor that functions as an adaptor for cullin-3-based E3 ligase to regulate proteasomal degradation of the antioxidant transcription factor NRF2.²¹ Mutations in several BTB/kelch family members are associated with human monogenic diseases; for example, monoallelic mutations in *KLHL3* (MIM: 605775) cause familial hyperkalemic

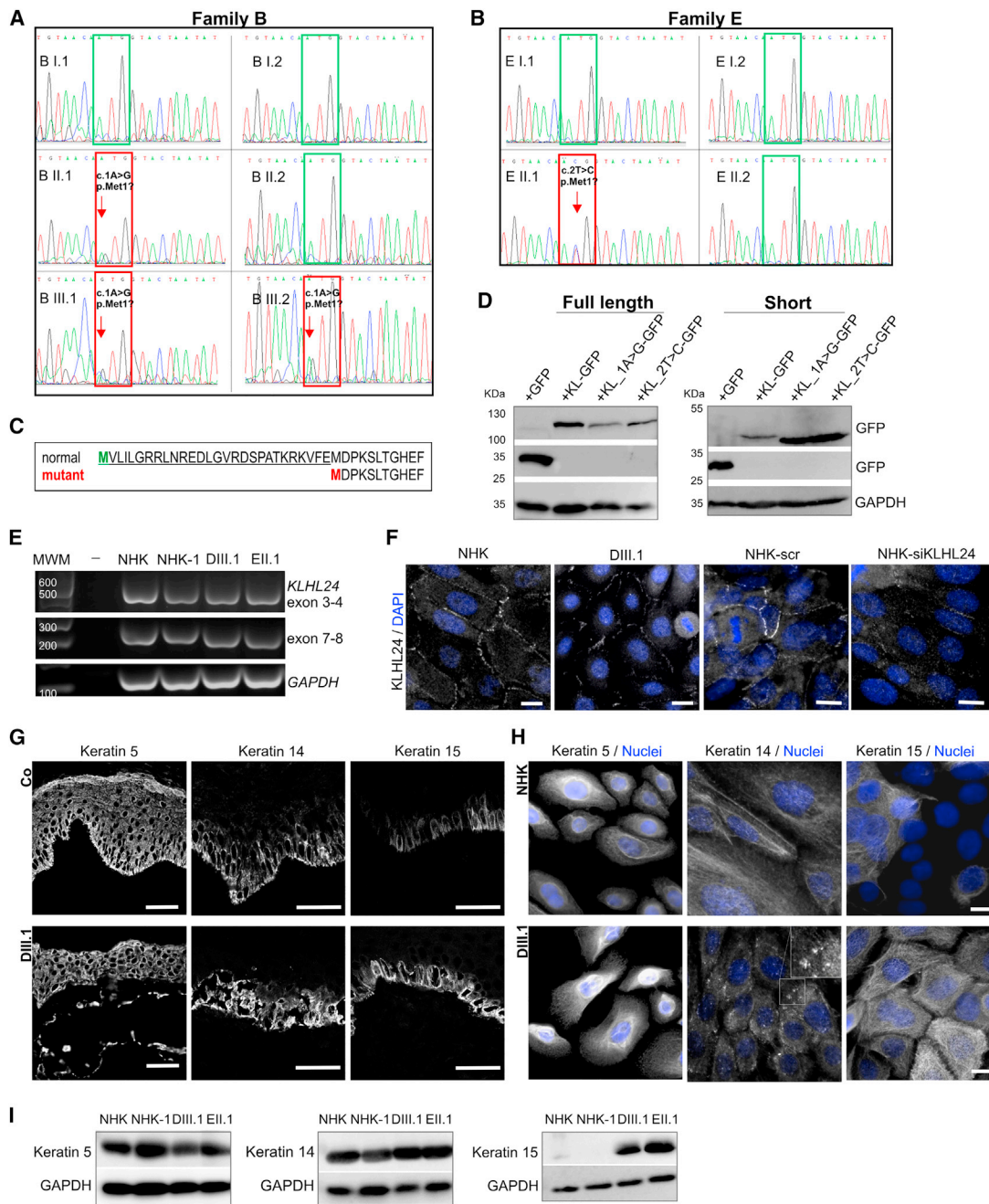


Figure 2. Mutations Affecting the Translation Initiation Codon of *KLHL24* and Their Consequences

(A and B) Sanger sequencing confirmed the *KLHL24* mutations and their segregation with the phenotype. Partial *KLHL24* sequences of members of families B (A) and E (B) are shown as examples. Note that in both families, the mutation occurred de novo.

(C) Schematic representation of the predicted usage of a downstream translation initiation codon due to the mutations.

(D) Recombinant expression of GFP-fused normal (KL-GFP) and mutant (KL_1A>G-GFP and KL_2T>C-GFP) full-length and short (cDNA sequence ending in exon 4) *KLHL24* polypeptides detected with antibodies to GFP demonstrates slightly faster migration of the mutants. The molecular weight is indicated on the left side in kDa. The pictures represent three technical and three biological replicates.

(E) RT-PCR with mRNA from keratinocytes of DIII.1 and EII.1 and normal human keratinocytes from two different donors (NHK and NHK-1) shows that *KLHL24* mRNA expression and splicing are not affected by the mutations of the start codon. RT-PCR with primers to *GAPDH* was run to control loading. Pictures represent experiments done with three biological replicates. MWM indicates the molecular-weight marker in base pairs.

(F) Distribution of *KLHL24* in the cytoplasm and at the periphery of normal human keratinocytes (NHK) and of keratinocytes treated with scramble siRNA. Staining intensity is reduced in keratinocytes treated with *KLHL24* specific siRNA and in DIII.1. Pictures represent three independent experiments. Scale bars represent 20 μ m.

(G and H) Immunostaining of keratins 5, 14, and 15 in skin samples (G) and in keratinocytes (H) from a normal control individual (Co and NHK) and from DIII.1. Inset in the middle lower panel of (H) is a 2-fold magnification of the marked area. Similar results were obtained with samples from the other individuals. Scale bars represent 50 μ m (G) and 20 μ m (H).

(I) Immunoblotting of whole-cell lysates with antibodies to keratins 5, 14, and 15. *GAPDH* antibodies were used to control loading.

hypertension (MIM: 614495), *KLHL7* (MIM: 611119) mutations are associated with retinitis pigmentosa (MIM: 612943), and *KLHL9* (MIM: 611201) mutations lead to autosomal-dominant distal myopathy.^{18,22–26} The kelch domain of *KLHL16* (or gigaxonin, encoded by *GAN* [MIM: 605379]) has been shown to interact with IF proteins affected in giant axonal neuropathy (MIM: 256850).²⁷ Gigaxonin, the substrate adaptor of an E3 ubiquitin ligase, emerged as the first IF regulator and is responsible for controlling the turnover of neurofilaments in addition to other IFs.^{28,29} The normal physiological role of gigaxonin is in the maintenance of cytoskeletal structures in normal tissues, including the processing of intermediate neural filaments in neural cells and vimentin in fibroblasts and endothelial cells.³⁰

Thus, we studied the expression of *KLHL24* in skin and skin cells. Normal human keratinocytes were cultured in keratinocyte growth medium (Invitrogen), and dermal fibroblasts were grown in DMEM supplemented with 10% FCS, 1% L-glutamine, and 1% pyruvate (Invitrogen). Human normal melanocytes were purchased from PromoCell and grown in melanocyte growth medium (PromoCell). RNA was isolated with the RNeasy Mini Kit (QIAGEN), transcribed into cDNA with the First Strand cDNA Synthesis Kit (Fermentas), and subjected to RT-PCR (primers are listed in Table S2). We found expression of *KLHL24* in all main skin cell types: keratinocytes, dermal fibroblasts, and melanocytes (Figure S3A). Next, immunofluorescence staining was performed on skin cryosections or on keratinocytes, which were seeded on coverslips, allowed to adhere and grow for 2 days, fixed with acetone and methanol, and processed as previously described³¹ (antibodies are listed in Table S3). In skin and keratinocytes, *KLHL24* was detected with a commercially available antibody (Abcam) intracellularly and at the cell periphery, where it partially colocalized with desmoplakin, a marker of desmosomes, and with E-cadherin, a component of adherens junctions (Figures S3B and S3C).

To assess the molecular consequences of *KLHL24* mutations, we generated cell lines from primary cells of individuals DIII.1 and EII.1 and control individuals by transduction with the HPV E6E7 genes (the construct was a kind gift from Dr. Fernando Larcher, and the helper plasmids were a gift from Dr. Stefanie Löffek) as described before.³² Mutations were confirmed in all cell lines (data not shown). As shown by RT-PCR, the mutations in the start codon of *KLHL24* did not result in reduced transcription or mRNA decay in keratinocytes or fibroblasts derived from the affected individuals (Figures 2E and S3D). Immunostaining of *KLHL24* demonstrated a different staining pattern between mutant keratinocytes (reduction of the signal in the cytoplasm and at the cell periphery) and normal human keratinocytes (Figure 2F). To validate the specificity of the antibody, we used normal human keratinocytes in which the expression of *KLHL24* had been knocked down by 75% (Figure S3E) with siRNA duplexes specific

to *KLHL24* (Table S4) (Eurogentec) and Lipofectamine 2000 (Invitrogen).

Like other kelch-like family members, *KLHL24* might be involved in protein ubiquitination, particularly the turnover of IF proteins, in a manner similar to that of gigaxonin. IF turnover is a highly dynamic process required for maintaining tissue integrity and is implicated in degenerative and regenerative processes.²⁹ Keratin IFs are crucial for maintaining cell and tissue integrity in that they act as structural scaffolds and are dynamic enough to sustain several additional processes. Keratins serve multiple homeostatic and stress-enhanced mechanical and non-mechanical functions in epithelia, including the maintenance of cellular integrity, regulation of cell growth and migration, and protection from apoptosis.³³ Keratin IFs display highly dynamic properties in response to injury, sometimes in the form of degradation of the keratin IF network.³⁴ Phosphorylation targets keratin proteins for degradation in these circumstances, and the turnover is regulated by the ubiquitin proteasome pathway.^{34–37}

To address the hypothesis that *KLHL24* mutations affect the degradation of keratins, we assessed keratins 5 and 14 in skin and cultured keratinocytes. Both keratins stained positive in skin sections of the individuals with *KLHL24* mutations, although cytolysis of basal keratinocytes was very often observed (Figure 2G). In cultured keratinocytes of the individuals with *KLHL24* mutations, keratin 14 staining (clones LL002 and EP1612Y) appeared disorganized, irregular, and fragmented, whereas keratin 5 (clone D5/16 B4 and polyclonal antibody), tubulin, and actin were not significantly changed (Figures 2H and S4A). The amounts of keratins 5 and 14 were 1.5- to 2-fold higher in whole-cell lysates³³ of *KLHL24* mutant keratinocytes than in control cells (Figure 2I). Similar results were obtained after fractionation of soluble and insoluble protein³³ (data not shown). Because keratin 15, a type I keratin present in minor amounts in basal keratinocytes, has been shown to form heterodimers with keratin 5³⁸ and have a compensatory effect on the skin of humans with keratin 14 variants,³⁹ we assessed the expression and abundance of keratin 15 (clone EPR1614Y) in the skin and keratinocytes of affected individuals and found a strong upregulation in comparison with control samples (Figures 2G–2I and S4B). All together, these findings suggest that mutations leading to N-terminal truncation of *KLHL24* affect basal epidermal keratins, in particular keratin 14.

Next, we used heat stress to challenge the keratin IFs and induce their disruption in keratinocytes.⁴⁰ In brief, cells were grown to subconfluence on coverslips, culture medium was replaced with prewarmed 43°C medium, and dishes were placed in a 43°C incubator for 15 min. Thereafter, the dishes were placed back at 37°C, and coverslips were fixed with ice-cold methanol and acetone, air-dried, blocked, and incubated with the primary antibodies. In the keratinocytes of the individuals with *KLHL24* mutations, the abnormalities of keratin 14 were

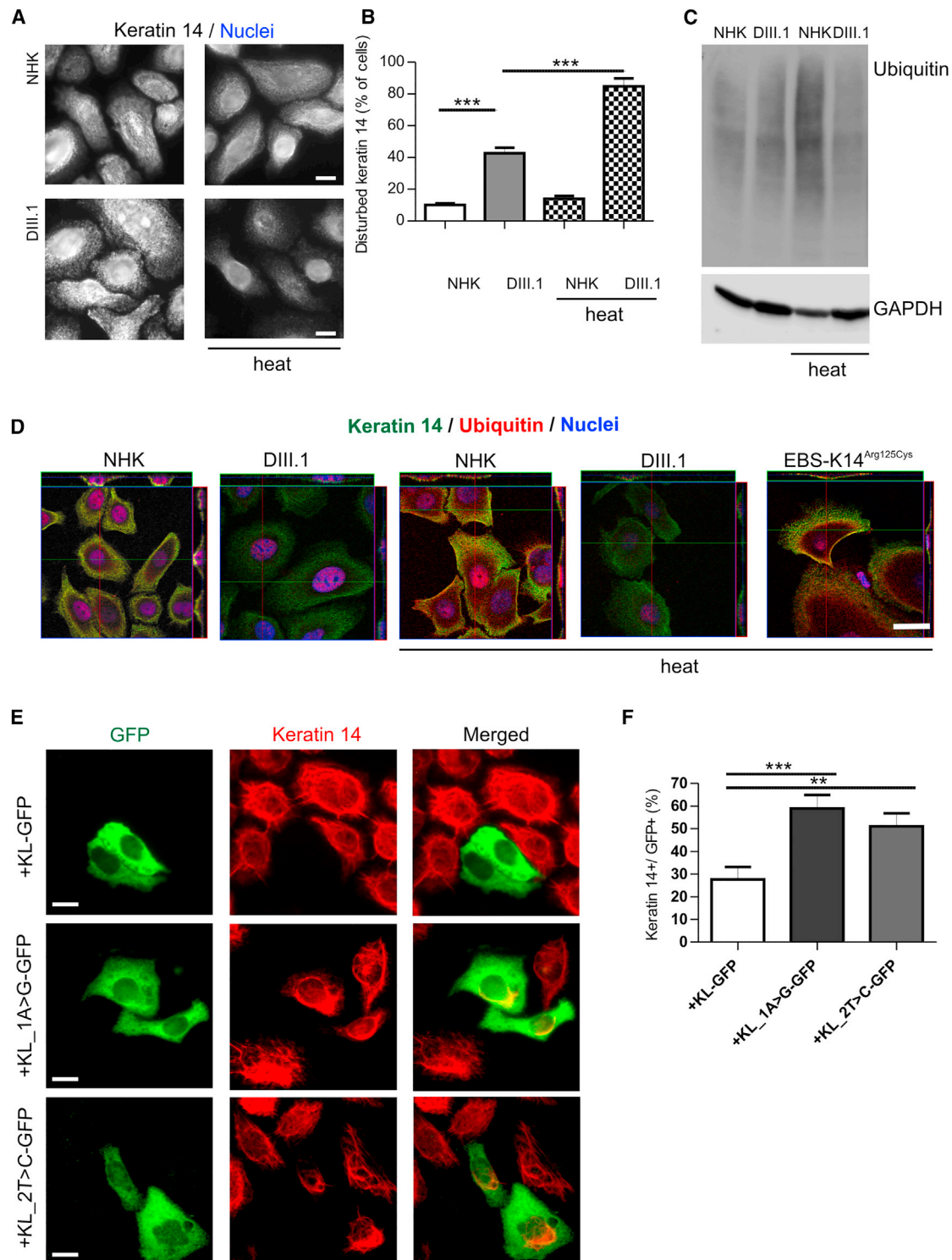


Figure 3. Alterations of Keratin 14 and Ubiquitin in *KLHL24* Mutant Cells

(A) Keratin 14 staining was disturbed in keratinocytes of DIII.1. After heat stress, remodeling (perinuclear distribution) and fragmentation of the keratin IFs was observed in the keratinocytes of DIII.1. Similar results were obtained with keratinocytes of EII.1. Scale bar represents 20 μ m.

(B) Quantification of the percentage of cells (mean values \pm SEM) with disturbed keratin 14 staining (10.10% \pm 1.05% of 270 NHK cells, 42.74% \pm 3.43% of 491 DIII.1 cells, 13.93% \pm 1.86% of 263 NHK + heat cells, and 84.8% \pm 5.01% of 407 DIII.1 + heat cells; *** p < 0.001). All data are from independent biological replicates, and statistical analysis was performed with an unpaired t test with Welch's correction.

(C) Immunoblots with lysates obtained from NHK and keratinocytes of DIII.1, with and without heat stress, were detected with antibodies to ubiquitin and GAPDH.

(legend continued on next page)

even more pronounced with perinuclear distribution and fragmentation, suggesting increased depolymerization⁴¹ after stress induction, whereas control cells changed very little (Figures 3A and 3B). The overall abundance of ubiquitinated proteins increased in control cells after heat stress but did not change significantly in the cells of the individuals with *KLHL24* mutations (Figures 3C and S4C). Confocal microscopy (LSM510, Carl Zeiss) showed that ubiquitin colocalized with keratin 14 in cells from a control individual and a person with EB simplex due to a mutation affecting keratin 14 (c.373C>T [p.Arg125Cys]). In contrast, in basal cell-culture conditions, particularly after heat stress, ubiquitin was not present in the cytoplasm and did not colocalize with keratin 14 in the cells of the individuals with *KLHL24* mutations (Figures 3D and S4C). Because stress-inducible kinase p38 was hyperactivated in keratinocytes from persons with EB simplex caused by mutations affecting keratin 5 or keratin 14 in basal culture conditions and further increased after osmotic or heat stress,^{42,43} we tested whether this was also the case in *KLHL24* mutant keratinocytes. We observed augmented phosphorylation of the stress-activated kinase p38 and, in line with this, an approximately 2-fold increase in the apoptosis (In Situ Cell Death Detection Kit, TMR red, Roche) of *KLHL24* mutant keratinocytes in basal cell-culture conditions and after heat stress (Figure S5). These results suggest that ubiquitination and subsequent proteasomal degradation of keratin 14 might be disturbed in the presence of the *KLHL24* mutations and thus result in cellular stress and apoptosis.

To directly address the effect of normal and mutant *KLHL24* on keratin 14 degradation, we assessed keratin 14 by immunofluorescence staining after recombinant overexpression of the GFP-tagged normal and mutant *KLHL24* cDNAs in HaCaT keratinocytes.⁴⁴ Of the cells overexpressing normal *KLHL24*, 72% were negative for keratin 14, supporting the hypothesis that, like gigaxolin,²⁸ *KLHL24* promotes IF degradation. In contrast, 41% of the cells expressing mutant *KLHL24* preserved the keratin 14 staining (Figures 3E and 3F), suggesting that the mutants have a lower ability to promote keratin 14 degradation than the normal molecule.

Finally, a broader role of *KLHL24* in the regulation of IFs is supported by the observation of fragmented vimentin IF in the fibroblasts of the individuals with *KLHL24* mutations, whereas the actin cytoskeleton always appeared normal (Figure S6).

We provide strong genetic data that imply mutations in the translation initiation codon of *KLHL24* as the cause of a distinct skin-fragility phenotype, which can be classified as EB simplex given the ultrastructural level of skin cleavage. Remarkably, mutation c.1A>G occurred de novo and was recurrent in families originating from different countries. The striking similarities of the clinical features point to a unique and very specific pathomechanism, which remains to be clarified in detail. In this regard, it is expected that nucleotide changes in the third position of the translation initiation codon (c.3G>A, c.3G>T, or c.3G>C) might also result in the same phenotype. We have shown that *KLHL24* is expressed in keratinocytes, dermal fibroblasts, and melanocytes (the main cells of the skin) and that it affects the ubiquitination and probably the proteasomal degradation of IFs, particularly keratin 14 in keratinocytes and vimentin in fibroblasts. Nevertheless, other targets and functions cannot be excluded.

The identified mutations lead to the formation of an N-terminally-truncated polypeptide that interferes with the physiological function of *KLHL24*, as shown by recombinant expression in HaCaT cells. The mutations do not alter *KLHL24* mRNA levels but rather change the protein amount and activity. Most data on the plasticity of the keratin network have been generated with cultured cells that overexpress fluorescence-tagged keratins, whereas the processes taking place in functional epithelial tissues remain largely unknown.⁴⁵ The abnormalities observed in authentic mutant keratinocytes include disorganization and fragmentation of keratin 14, which was more abundant than in control cells, suggesting an abnormal degradation. In the skin, where IF turnover is much lower than in cell culture, the anomalies demonstrated by immunostaining and TEM were mainly associated with cytolysis of the basal keratinocytes.

The in vivo turnover of keratins is critical during development, when active cell division takes place in response to environmental stressors, and probably during differentiation of basal keratinocytes to the suprabasal layer. The observed anomalies of keratin 14 might correlate with the pronounced skin fragility at birth and the spontaneous alleviation in adulthood, noted in the *KLHL24*-mutation-affected individuals examined in this study. Upregulation of keratin 15 might also contribute to the keratin network in mutant keratinocytes, but keratin 5 and keratin 15 filaments cannot provide sufficient mechanical strength to withstand physical trauma.³⁸ We noted both certain

(D) Confocal z stack images of the keratinocytes stained with keratin 14 and ubiquitin antibodies demonstrate colocalization of these markers in the cytoplasm of normal human keratinocytes or keratinocytes of a person with EB simplex due to the keratin 14 variant p.Arg125Cys (EBS-K14^{R125C}). In the keratinocytes of DIII.1, ubiquitin did not demonstrate any cytoplasmic localization. Scale bar represents 20 μ m.

(E) HaCat cells were transfected with the normal (KL-GFP) and mutant *KLHL24* cDNAs (KL_1A>G-GFP and KL_2T>C-GFP) and stained with antibodies to keratin 14 (red) and GFP (green). Scale bars represent 20 μ m.

(F) The graph represents the percentage of keratin-14-positive cells (mean values \pm SEM) among those expressing recombinant normal (KL-GFP) or mutant *KLHL24* cDNAs (27.66% \pm 5.48% of 166 KL-GFP cells, 58.94% \pm 5.89% of 120 KL_1A>G-GFP cells, and 51.12% \pm 5.63% of 147 KL_2T>C-GFP cells; ***p < 0.001 and **p < 0.01). Data are from three independent experiments. Statistical analysis was performed with an unpaired t test with Welch's correction.

similarities and differences between the biological phenotypes of keratinocytes with mutations affecting *KLHL24* and keratin 14. Of particular interest is the increased p38 phosphorylation observed in *KLHL24* mutant keratinocytes. It was reported that phosphorylated p38 colocalized with keratin during mitosis in various stress situations and in cells producing mutant keratins. In all of these situations, keratin 8 became phosphorylated on Ser73, a well-known p38 target site. The p38-dependent signaling is a major intermediate-filament-regulating pathway with rapid and reversible effects on keratin phosphorylation and organization in diverse physiological, stress, and pathological situations.^{6,46}

Nevertheless, the distinct phenotype associated with *KLHL24* mutations does not overlap the clinical pictures observed in individuals with EB simplex (MIM: 131760, 131900, 601001, and 131800) due to dominant missense or recessive null mutations affecting keratin 14¹ or in individuals with Naegeli syndrome (MIM: 161000) due to keratin 14 haploinsufficiency.⁴⁷ The particular features of this phenotype (skin atrophy and scarring) could be explained by increased apoptosis of the keratinocytes, by anomalies of the fibroblasts' IFs, and by additional functions of *KLHL24*.

Accession Numbers

The accession number for the data reported in this paper is ClinVar: SCV000328619.

Supplemental Data

Supplemental Data include six figures and four tables and can be found with this article online at <http://dx.doi.org/10.1016/j.ajhg.2016.11.005>.

Acknowledgments

The research was funded by a grant (Has 1) from Debra International to C.H. Y.H. was partially supported by Collaborative Research Centre 1140. We thank the families for their participation; Leena Bruckner-Tuderman for critical reading of the manuscript and discussions; Amelie Höninger, Gabriele Grüninger, Amelie Gruler, Käthe Thoma, Vera Morand, and Jannis Athanasios for excellent support; Dr. Fernando Larcher (CIEMAT-CIBER, Madrid, Spain) for the E6E7 construct; Dr. Stefanie Löffek for reagents; Dr. Jürgen Kohlhase (Center for Human Genetics Freiburg); BGI Genomics for sequencing; and the Life Imaging Center's Center for Biological Systems Analysis (ZBSA) of the Albert-Ludwigs-University microscopy platform for excellent support.

Received: October 14, 2016

Accepted: November 7, 2016

Published: November 23, 2016

Web Resources

1000 Genomes, <http://www.1000genomes.org>
ClinVar, <https://www.ncbi.nlm.nih.gov/clinvar/>

ExAC Browser, <http://exac.broadinstitute.org/>
MutationTaster, <http://www.mutationtaster.org/>
NHLBI Exome Sequencing Project (ESP) Exome Variant Server, <http://evs.gs.washington.edu/EVS/>
OMIM, <http://www.omim.org/>
RefSeq, <http://www.ncbi.nlm.nih.gov/RefSeq>
UCSC Genome Browser, <http://genome.ucsc.edu>

References

1. Fine, J.-D., Bruckner-Tuderman, L., Eady, R.A.J., Bauer, E.A., Bauer, J.W., Has, C., Heagerty, A., Hintner, H., Hovnanian, A., Jonkman, M.F., et al. (2014). Inherited epidermolysis bullosa: updated recommendations on diagnosis and classification. *J. Am. Acad. Dermatol.* *70*, 1103–1126.
2. Has, C., and Bruckner-Tuderman, L. (2014). The genetics of skin fragility. *Annu. Rev. Genomics Hum. Genet.* *15*, 245–268.
3. Bolling, M.C., Lemmink, H.H., Jansen, G.H.L., and Jonkman, M.F. (2011). Mutations in *KRT5* and *KRT14* cause epidermolysis bullosa simplex in 75% of the patients. *Br. J. Dermatol.* *164*, 637–644.
4. Rugg, E.L., Horn, H.M., Smith, F.J., Wilson, N.J., Hill, A.J.M., Magee, G.J., Shemanko, C.S., Baty, D.U., Tidman, M.J., and Lane, E.B. (2007). Epidermolysis bullosa simplex in Scotland caused by a spectrum of keratin mutations. *J. Invest. Dermatol.* *127*, 574–580.
5. Kopečková, L., Bučková, H., Kýrová, J., Gaillyová, R., Němečková, J., Jeřábková, B., Veselý, K., Stehlíková, K., and Fajkusová, L. (2016). Ten years of DNA diagnostics of epidermolysis bullosa in the Czech Republic. *Br. J. Dermatol.* *174*, 1388–1391.
6. Loschke, F., Seltmann, K., Bouameur, J.E., and Magin, T.M. (2015). Regulation of keratin network organization. *Curr. Opin. Cell Biol.* *32*, 56–64.
7. McGrath, J.A., Stone, K.L., Begum, R., Simpson, M.A., Dopping-Hepenstal, P.J., Liu, L., McMillan, J.R., South, A.P., Pourreya, C., McLean, W.H., et al. (2012). Germline Mutation in *EXPH5* Implicates the Rab27B Effector Protein *Slac2-b* in Inherited Skin Fragility. *Am. J. Hum. Genet.* *91*, 1115–1121.
8. Bolling, M.C., Jongbloed, J.D.H., Boven, L.G., Diercks, G.F.H., Smith, F.J.D., McLean, W.H.L., and Jonkman, M.F. (2014). Plectin mutations underlie epidermolysis bullosa simplex in 8% of patients. *J. Invest. Dermatol.* *134*, 273–276.
9. Groves, R.W., Liu, L., Dopping-Hepenstal, P.J., Markus, H.S., Lovell, P.A., Ozoemena, L., Lai-Cheong, J.E., Gawler, J., Owaribe, K., Hashimoto, T., et al. (2010). A homozygous nonsense mutation within the dystonin gene coding for the coiled-coil domain of the epithelial isoform of *BPAG1* underlies a new subtype of autosomal recessive epidermolysis bullosa simplex. *J. Invest. Dermatol.* *130*, 1551–1557.
10. Has, C., and He, Y. (2016). Research Techniques Made Simple: Immunofluorescence Antigen Mapping in Epidermolysis Bullosa. *J. Invest. Dermatol.* *136*, e65–e71.
11. Li, H., and Durbin, R. (2009). Fast and accurate short read alignment with Burrows-Wheeler transform. *Bioinformatics* *25*, 1754–1760.
12. Van der Auwera, G.A., Carneiro, M.O., Hartl, C., Poplin, R., Del Angel, G., Levy-Moonshine, A., Jordan, T., Shakir, K., Roazen, D., Thibault, J., et al. (2013). From FastQ data to high confidence variant calls: the Genome Analysis Toolkit best

- practices pipeline. *Curr. Protoc. Bioinformatics* 43, 11.10.1–11.10.33.
13. Schwarz, J.M., Cooper, D.N., Schuelke, M., and Seelow, D. (2014). MutationTaster2: mutation prediction for the deep-sequencing age. *Nat. Methods* 11, 361–362.
 14. Laezza, F., Wilding, T.J., Sequeira, S., Coussen, F., Zhang, X.Z., Hill-Robinson, R., Mülle, C., Huettner, J.E., and Craig, A.M. (2007). KRIP6: a novel BTB/kelch protein regulating function of kainate receptors. *Mol. Cell. Neurosci.* 34, 539–550.
 15. Laezza, F., Wilding, T.J., Sequeira, S., Craig, A.M., and Huettner, J.E. (2008). The BTB/kelch protein, KRIP6, modulates the interaction of PICK1 with GluR6 kainate receptors. *Neuropharmacology* 55, 1131–1139.
 16. Stogios, P.J., Downs, G.S., Jauhal, J.J.S., Nandra, S.K., and Privé, G.G. (2005). Sequence and structural analysis of BTB domain proteins. *Genome Biol.* 6, R82.
 17. Prag, S., and Adams, J.C. (2003). Molecular phylogeny of the kelch-repeat superfamily reveals an expansion of BTB/kelch proteins in animals. *BMC Bioinformatics* 4, 42.
 18. Dhanoa, B.S., Cogliati, T., Satish, A.G., Bruford, E.A., and Friedman, J.S. (2013). Update on the Kelch-like (KLHL) gene family. *Hum. Genomics* 7, 13.
 19. Xu, L., Wei, Y., Reboul, J., Vaglio, P., Shin, T.-H., Vidal, M., Elledge, S.J., and Harper, J.W. (2003). BTB proteins are substrate-specific adaptors in an SCF-like modular ubiquitin ligase containing CUL-3. *Nature* 425, 316–321.
 20. Furukawa, M., He, Y.J., Borchers, C., and Xiong, Y. (2003). Targeting of protein ubiquitination by BTB-Cullin 3-Roc1 ubiquitin ligases. *Nat. Cell Biol.* 5, 1001–1007.
 21. Kobayashi, A., Kang, M.-I., Okawa, H., Ohtsui, M., Zenke, Y., Chiba, T., Igarashi, K., and Yamamoto, M. (2004). Oxidative stress sensor Keap1 functions as an adaptor for Cul3-based E3 ligase to regulate proteasomal degradation of Nrf2. *Mol. Cell. Biol.* 24, 7130–7139.
 22. Louis-Dit-Picard, H., Barc, J., Trujillano, D., Miserey-Lenkei, S., Bouatia-Naji, N., Pylypenko, O., Beaurain, G., Bonnefond, A., Sand, O., Simian, C., et al.; International Consortium for Blood Pressure (ICBP) (2012). KLHL3 mutations cause familial hyperkalemic hypertension by impairing ion transport in the distal nephron. *Nat. Genet.* 44, 456–460, S1–S3.
 23. Boyden, L.M., Choi, M., Choate, K.A., Nelson-Williams, C.J., Farhi, A., Toka, H.R., Tikhonova, I.R., Bjornson, R., Mane, S.M., Colussi, G., et al. (2012). Mutations in kelch-like 3 and cullin 3 cause hypertension and electrolyte abnormalities. *Nature* 482, 98–102.
 24. Friedman, J.S., Ray, J.W., Waseem, N., Johnson, K., Brooks, M.J., Hugosson, T., Breuer, D., Branham, K.E., Krauth, D.S., Bowne, S.J., et al. (2009). Mutations in a BTB-Kelch protein, KLHL7, cause autosomal-dominant retinitis pigmentosa. *Am. J. Hum. Genet.* 84, 792–800.
 25. Angius, A., Uva, P., Buers, I., Oppo, M., Puddu, A., Onano, S., Persico, I., Loi, A., Marcia, L., Höhne, W., et al. (2016). Biallelic Mutations in KLHL7 Cause a Crisponi/CISS1-like Phenotype Associated with Early-Onset Retinitis Pigmentosa. *Am. J. Hum. Genet.* 99, 236–245.
 26. Cirak, S., von Deimling, F., Sachdev, S., Errington, W.J., Herrmann, R., Bönnemann, C., Brockmann, K., Hinderlich, S., Lindner, T.H., Steinbrecher, A., et al. (2010). Kelch-like homologue 9 mutation is associated with an early onset autosomal dominant distal myopathy. *Brain* 133, 2123–2135.
 27. Johnson-Kerner, B.L., Garcia Diaz, A., Ekins, S., and Wichterle, H. (2015). Kelch Domain of Gigaxonin Interacts with Intermediate Filament Proteins Affected in Giant Axonal Neuropathy. *PLoS ONE* 10, e0140157.
 28. Mahammad, S., Murthy, S.N.P., Didonna, A., Grin, B., Israeli, E., Perrot, R., Bomont, P., Julien, J.-P., Kuczumski, E., Opal, P., and Goldman, R.D. (2013). Giant axonal neuropathy-associated gigaxonin mutations impair intermediate filament protein degradation. *J. Clin. Invest.* 123, 1964–1975.
 29. Bomont, P. (2016). Degradation of the Intermediate Filament Family by Gigaxonin. *Methods Enzymol.* 569, 215–231.
 30. Kang, J.J., Liu, I.Y., Wang, M.B., and Srivatsan, E.S. (2016). A review of gigaxonin mutations in giant axonal neuropathy (GAN) and cancer. *Hum. Genet.* 135, 675–684.
 31. He, Y., Esser, P., Heinemann, A., Bruckner-Tuderman, L., and Has, C. (2011). Kindlin-1 and -2 have overlapping functions in epithelial cells implications for phenotype modification. *Am. J. Pathol.* 178, 975–982.
 32. Yalcin, E.G., He, Y., Orhan, D., Pazzagli, C., Emiralioglu, N., and Has, C. (2015). Crucial role of posttranslational modifications of integrin $\alpha 3$ in interstitial lung disease and nephrotic syndrome. *Hum. Mol. Genet.* 24, 3679–3688.
 33. Wang, F., Ziemann, A., and Coulombe, P.A. (2016). Skin Keratins. *Methods Enzymol.* 568, 303–350.
 34. Rogel, M.R., Jaitovich, A., and Ridge, K.M. (2010). The role of the ubiquitin proteasome pathway in keratin intermediate filament protein degradation. *Proc. Am. Thorac. Soc.* 7, 71–76.
 35. Ridge, K.M., Linz, L., Flitney, F.W., Kuczumski, E.R., Chou, Y.-H., Omary, M.B., Sznajder, J.I., and Goldman, R.D. (2005). Keratin 8 phosphorylation by protein kinase C delta regulates shear stress-mediated disassembly of keratin intermediate filaments in alveolar epithelial cells. *J. Biol. Chem.* 280, 30400–30405.
 36. Jaitovich, A., Mehta, S., Na, N., Ciechanover, A., Goldman, R.D., and Ridge, K.M. (2008). Ubiquitin-proteasome-mediated degradation of keratin intermediate filaments in mechanically stimulated A549 cells. *J. Biol. Chem.* 283, 25348–25355.
 37. Sivaramakrishnan, S., Schneider, J.L., Sitikov, A., Goldman, R.D., and Ridge, K.M. (2009). Shear stress induced reorganization of the keratin intermediate filament network requires phosphorylation by protein kinase C zeta. *Mol. Biol. Cell* 20, 2755–2765.
 38. Lloyd, C., Yu, Q.C., Cheng, J., Turksen, K., Degenstein, L., Hutton, E., and Fuchs, E. (1995). The basal keratin network of stratified squamous epithelia: defining K15 function in the absence of K14. *J. Cell Biol.* 129, 1329–1344.
 39. Jonkman, M.F., Heeres, K., Pas, H.H., van Luyn, M.J., Elema, J.D., Corden, L.D., Smith, F.J., McLean, W.H., Ramaekers, F.C., Burton, M., and Scheffer, H. (1996). Effects of keratin 14 ablation on the clinical and cellular phenotype in a kindred with recessive epidermolysis bullosa simplex. *J. Invest. Dermatol.* 107, 764–769.
 40. Tan, T.S., Ng, Y.Z., Badowski, C., Dang, T., Common, J.E.A., Lacina, L., Szeverényi, I., and Lane, E.B. (2016). Assays to Study Consequences of Cytoplasmic Intermediate Filament Mutations: The Case of Epidermal Keratins. *Methods Enzymol.* 568, 219–253.
 41. Moch, M., Herberich, G., Aach, T., Leube, R.E., and Windoffer, R. (2013). Measuring the regulation of keratin filament network dynamics. *Proc. Natl. Acad. Sci. USA* 110, 10664–10669.
 42. Chamcheu, J.C., Navsaria, H., Pihl-Lundin, I., Liovic, M., Vahlquist, A., and Törmä, H. (2011). Chemical chaperones

- protect epidermolysis bullosa simplex keratinocytes from heat stress-induced keratin aggregation: involvement of heat shock proteins and MAP kinases. *J. Invest. Dermatol.* *131*, 1684–1691.
43. Liovic, M., Lee, B., Tomic-Canic, M., D'Alessandro, M., Bolshakov, V.N., and Lane, E.B. (2008). Dual-specificity phosphatases in the hypo-osmotic stress response of keratin-defective epithelial cell lines. *Exp. Cell Res.* *314*, 2066–2075.
 44. Boukamp, P., Petrussevska, R.T., Breitkreutz, D., Hornung, J., Markham, A., and Fusenig, N.E. (1988). Normal keratinization in a spontaneously immortalized aneuploid human keratinocyte cell line. *J. Cell Biol.* *106*, 761–771.
 45. Schwarz, N., Windoffer, R., Magin, T.M., and Leube, R.E. (2015). Dissection of keratin network formation, turnover and reorganization in living murine embryos. *Sci. Rep.* *5*, 9007.
 46. Wöll, S., Windoffer, R., and Leube, R.E. (2007). p38 MAPK-dependent shaping of the keratin cytoskeleton in cultured cells. *J. Cell Biol.* *177*, 795–807.
 47. Lugassy, J., Itin, P., Ishida-Yamamoto, A., Holland, K., Huson, S., Geiger, D., Hennies, H.C., Indelman, M., Bercovich, D., Uitto, J., et al. (2006). Naegeli-Franceschetti-Jadassohn syndrome and dermatopathia pigmentosa reticularis: two allelic ectodermal dysplasias caused by dominant mutations in KRT14. *Am. J. Hum. Genet.* *79*, 724–730.